1 **Interactive climate factors restrict future increases in spring tree productivity**

2

3 **Running title: Future constraints on earlier spring arrival**

4

5 Authors: Constantin M. Zohner*[1], Lidong Mo[1], Thomas A.M. Pugh[2,3], Jean-Francois Bastin[1],

6 and Thomas W. Crowther[1]

7

8 **Affiliations:**

9 [1]Institute of Integrative Biology, ETH Zurich (Swiss Federal Institute of Technology),

10 Universitätsstrasse 16, 8092 Zurich, Switzerland

11 [2]School of Geography, Earth and Environmental Sciences, University of Birmingham,

12 Edgbaston, Birmingham, B15 2TT, UK

13 [3]Birmingham Institute of Forest Research, University of Birmingham, Edgbaston, Birmingham,

14 B15 2TT, UK

15

16 *Author for correspondence: constantin.zohner@t-online.de

17

21

27 **Abstract**

28 Climate warming is currently advancing spring leaf-out, enhancing net primary productivity

29 (NPP) of temperate forests. However, it remains unclear whether this trend will continue. Using

30 727,401 direct phenological observations of dominant forest trees, we test for the major controls

31 on leaf-out and forecast future trajectories of spring arrival. By representing hypothesized

32 relationships with day-length, autumn temperature and winter-chilling, we accurately predicted

33 reductions in the advance of leaf-out. There was a strong consensus between our empirical

34 model and existing process-based models, revealing that the advance in leaf-out will not exceed

35 2 weeks over the rest of century. By incorporating these trends into a dynamic global vegetation

36 model, we estimate that these environmental constraints reduce the expected increases in forest

37 NPP by ~0.6 Gt per year. These findings reveal important environmental constraints on the

38 productivity of broadleaf deciduous trees and highlight that shifting spring phenology is

39 unlikely to slow the rate of warming by offsetting anthropogenic carbon emissions.

40

41 Keywords: Climate change, Phenology, Spring leaf-out, Carbon cycle

42

43

44

45

46

47

48

49

50

51

52

Main text

Shifts in the timing of annual growth cycles in temperate trees have direct impacts on global biogeochemical cycles[1–3], species distribution patterns[4], and ultimately feedback to the climate system by affecting the atmospheric carbon budget[2]. There is broad consensus that warming trends over the past decades have led to an earlier arrival of spring leaf emergence in Northern Hemisphere temperate trees, a trend that is enhancing global primary productivity under climate change[1,5,6]. Depending on species and location, leaf emergence has advanced by 3–8 days for every degree increase in air temperature[5–7]. However, a growing body of evidence suggests that this past trend cannot be used to predict future responses, because other environmental factors may constrain the future advances in spring phenology[8–11]. Aside from spring temperature, most temperate trees rely on additional factors including winter chilling and day-length, that are likely to become limiting in the future[8–11]. Yet, a lack of information about the existence, or relative importance of these drivers translates to high uncertainty in model predictions of future forest phenology[12]. Given that each day advance in spring leaf unfolding of deciduous trees translates to an increase in net ecosystem carbon uptake of 4.5 gC m^{-2} (ref [1]), untangling these mechanisms is critical for improving confidence in future climate projections.

Three main factors — autumn temperatures[13,14], winter chilling[8,10,15,16], and day length[17–19] — have been proposed to control spring leaf-out by modulating the amount of warming that trees require to leaf-out. Each of these factors is likely to counteract the advances in spring onset under a warming climate. Specifically, as the climate warms, the accumulated warming required for leaves to emerge is expected to increase because: (i) warmer autumn temperatures delay the initiation of dormancy[13,14]; (ii) warmer winters lead to reduced chilling accumulation[6,20]; and (iii) days at spring onset are becoming shorter[17,21–23] (Fig. 1). The potential effects of these separate environmental drivers have been identified using controlled climate chamber experiments with pot plants or twig cuttings[9–11]. These studies provide valuable mechanistic insights, but they do not necessarily reflect the behavior of mature trees

79 under natural growing conditions[24]. Although the inclusion of these hypothesized mechanisms

80 can improve the performance of mechanistic phenological models, the exact nature, and relative

81 importance, of these mechanisms remains untested under natural conditions[23]. As such, we

82 cannot represent these mechanisms in global biogeochemical models to predict the

83 consequences for future temperate forest productivity. Parameterizing phenological models and

84 translating their effects into global biogeochemical models requires direct empirical evidence

85 about the effects of these dominant environmental drivers in mature trees exposed to real-world

86 changes in natural environmental conditions[25].

87   To represent the important phenological mechanisms into larger biogeochemical

88 models, we need unifying evidence for the strength and direction of these ecological

89 parameters. Empirically testing the influence of these environmental constraints is also vital for

90 avoiding overparameterization in global biogeochemical models, which need to rely on simple

91 sub-models to represent plant physiological processes. To date, dynamic global vegetation

92 models, such as LPJ-GUESS, cannot reflect the complex dynamics that are represented in

93 specialized phenology models. As such, they can only account for spring phenology using a

94 simple degree-day–chilling relationship, neglecting the important physiological mechanisms

95 that are likely to restrict the advance of spring phenology in the future. These models are thus

96 likely to vastly overestimate the advances in spring phenology over the rest of the century.

97 Addressing this huge source of uncertainty necessitates that we generate simple empirical

98 parameters for the combined roles of autumn temperature, winter chilling and day length.

99   In this study, we aim to bridge the gap between specialized phenological models and

100 global vegetation models by developing a simple, empirical model to evaluate the key

101 mechanisms represented in process-based models. Using a massive *in situ* database of forest

102 leaf-out observations, we determine the interactive effects of autumn temperature, winter

103 chilling and spring day-length variation on thermal requirements to leaf-out in mature temperate

104 forest trees. We then use the observed relationships to train statistical predictions of future

105   spring arrival. By comparing this empirical model performance with all available process-based

106   models from the phenological literature, we show that it adequately reflects the dominant

107   drivers of spring phenology, and predicts spring leaf-out with as much accuracy as existing

108   mechanistic models. In addition, we use forecasts of future temperatures to project the future

109   changes in spring phonology under two climate change scenarios ("CO_2 stabilization" scenario,

110   RCP 4.5 and "business-as-usual", RCP 8.5). With high confidence in our 'simple' empirical

111   model performance, we could then use the calculated coefficients to train a global dynamic

112   vegetation model to more accurately reflect the future changes in spring phenology. Ultimately,

113   this big-data approach enables us to test the effects of interacting climate drivers, benchmark

114   model projections, and evaluate how these mechanisms influence global dynamic vegetation

115   model predictions of future phenology and global net primary productivity (NPP).

116

117   **Empirical test of the environmental drivers of spring leaf-out**

118   This analysis is underpinned by a massive database of *in situ* observations of leaf-out

119   date in mature individuals of nine temperate tree species that dominate European forests,

120   collected from the Pan European Phenology Project[26] – the only database to date, that contains

121   long-term (>15 years), ground-sourced phenological observations. After initial filtering, we

122   obtained 24,650 individual data series (lasting between 15 and 63 years) from 4,165 locations

123   across Central Europe (Fig. S1), resulting in 727,401 observations across all timeseries (see

124   Methods). To test for the importance of autumn temperatures, winter chilling, and spring day-

125   length on warming required to leaf-out at each site, we applied univariate regression models

126   over time at the individual-level (Fig. 2). Winter chilling, reflecting the sum of chilling from 1

127   October until the mean leaf-out date of each individual, was calculated in two ways (either

128   temperatures below 5 °C, or between 0 – 5 °C) to reflect two possibilities proposed in the

129   literature[20,27,28]. To calculate the day-length perceived by plants at the time when spring

130   warming occurs for each year, we first needed to define a date reflecting the onset of spring

131   warming. To do so, for each site and species combination, we calculated the average degree-

132   days accumulating before leaf-out. Spring onset each year was then defined as the date when

133   the average degree-days to leaf-out at the respective site were reached. We then transformed

134   this date to the corresponding day length value. This "day length value" thus reflects how early

135   spring warming occurred each year.

136   Before building our multivariate *full model,* we applied linear univariate models to test

137   for the separate effects of each environmental variable. These models showed that, while

138   autumn temperatures had a relatively minor effect, both winter chilling ($P < 0.001$; Correlation

139   coefficient $= 0.4 - 0.5$) and day-length ($P < 0.001$; Correlation coefficient $= 0.5 - 0.7$) had

140   consistent negative effects on accumulated warming required to leaf-out across all species

141   (Figs. 2 and S2). Interestingly, when chilling was calculated using all temperatures below 5°C,

142   the model outperformed an equivalent model in which effective chilling temperatures range

143   between 0 and 5°C, a commonly used approach[7,27] (Fig. 2b). In line with previous studies[9,17,21],

144   European beech showed the strongest chilling and day length sensitivity (Fig. 2b, c), but the

145   limiting effects of both variables were consistent across all temperate tree species. Consistent

146   with the findings of a previous study[30], these results show that the timing of the onset of spring

147   warming represents a strong control on leaf-out. See ref[30] for a more detailed test of this

148   relationship. It is also possible that this time effect could ultimately be driven by mechanisms

149   other than day length, such as an internal clock or changes in spectral light composition[31]. Our

150   results do not give mechanistic insights that would allow us to disentangle the mechanisms by

151   which plants sense the time of the year, but they provide important evidence that both winter

152   chilling and the timing of the onset of spring warming modulate the amount of warming

153   required to leaf-out, thereby restricting future responses to climate change.

154   To predict the amount of warming required for each tree to leaf-out, we then ran

155   multivariate models, including all three factors (autumn temperature, winter chilling, and day

156   length) and the interactions between them. The best model (lowest AIC and highest R^2) included

157   chilling and day length as fixed effects, and an interaction between winter chilling and day

158   length (Fig. S3a). This interaction term is supported by experimental studies showing that

159   winter chilling can substitute for day length and *vice versa*[9,10,17,18,22]. Across all species, the full

160   model accurately predicted the accumulated warming required to leaf-out across 727,401

161   observations over 63 years (R^2 values ranging between 0.4 and 0.6; Fig. S3a). As such, the

162   coefficients in these empirical models reveal parameters for each of the dominant

163   environmental drivers of spring phenology that are necessary for predicting changes in leaf-out

164   over time.

165   To test for the importance of these ecological mechanisms, we compared the predictions

166   of our *full model* (with spring warming, day length, and winter chilling) against similar

167   empirical models that lack these mechanisms. Specifically, we compared the performance of

168   our *full-model* to a simple *"null model"*, which included only spring warming, and a "c*hilling*

169   *model"* (see equation 7) – including spring warming and winter chilling – which has previously

170   been implemented in the LPJ-GUESS dynamic global vegetation model. By contrast to more

171   complex phenological models, the starting date of degree-day accumulation was not fitted to

172   the observed data and instead fixed to the first day of the year, allowing for easy incorporation

173   into large-scale vegetation models. This also ensures that the *null model* (warming-only model)

174   is not confounded by other factors because fitting a starting date of degree-day accumulation

175   implicitly accounts for winter chilling and/or day-length by determining when plants become

176   susceptible to spring warming. On average, across all species in our dataset, observed leaf-out

177   dates advanced by 3.8 ± 0.1 days per each degree increase in air temperature. The *full model*

178   performed well in predicting this temperature sensitivity, predicting 3.7 ± 0.2 days/°C. In

179   contrast, because they lack the ecological mechanisms that might restrict future advances in

180   spring leaf-out, the *chilling* and *null model* over-estimated leaf emergence, predicting 4.9 ± 0.2

181   and 6.3 ± 0.2 days/°C, respectively (Fig. 3b). The inclusion of all three mechanisms vastly

182   improved model accuracy. But more importantly, this reduced the over-estimation of spring

183 leaf-emergence in extremely warm years. This demonstrates that the combined roles of winter

184 chilling, day length, and spring warming need to be accounted for in predictions of future tree

185 phenology and productivity.

186

187 **Evaluating phenology model performance**

188   To evaluate whether our full empirical model (the *full model*) is capturing the

189 mechanisms in existing state-of-the-art phenology models, we compared the performance of

190 our full model against 17 process models from the literature (Fig. 4). We stress that, even though

191 some of these models are called "ecodormancy models" (suggesting that they solely consider

192 spring warming as a factor), all of these models at least implicitly account for winter chilling-

193 / day length-induced endodormancy release by fitting specific starting dates of degree-day

194 accumulation to the data (we therefore refer to them as explicit or implicit endodormancy

195 models hereafter). Although fitting a specific starting date of degree-day accumulation cannot

196 reflect the gradual transition from endo- to ecodormancy (see e.g. Fig. 2 in ref[22]), these models

197 all directly or indirectly represent the ecological mechanisms that we have evaluated in our *full*

198 *model*.

199   Compared to all existing phenology models, our empirical model performed well in

200 predicting leaf emergence over the last 15 years of leaf-out observations. Explaining over 50%

201 of the variation in spring leaf emergence over 727,401 observations, our simple model

202 performed well. This was only marginally worse explanatory power than the best available

203 phenology models (RMSE values) (Fig. 4c). But most importantly, our *full model* excelled in

204 terms of model-accuracy, with predictions fitting close to the 1:1 line in predicted *vs.* observed

205 plots, compared to most other models (Fig. 4c). That is, the intercept and slope components of

206 observed *vs.* predicted comparisons of leaf-out dates for our *full model* were among the least

207 likely to differ from 1 and 0, respectively, with a significant (P <0.05) deviation only found for

208 <2% of sites (Fig. 4 a,b). Four of the other process-based models showed an equally low

209   proportion of significant sites with exceptionally high model accuracy. Model accuracy was

210   slightly lower for 11 models (2–6% significant sites), while the remaining 4 models all

211   performed considerably worse (13–88% significant sites) [Fig. 4 a,b].

212   The high predictive accuracy of the top 4 process models is in direct contrast with

213   previous studies, which suggested low performance across all phenology models[12]. This

214   distinction is likely to arise from our focus on model accuracy (i.e. slope estimates) rather than

215   model fit (i.e. root mean squared error), and the test if predicted values (in the x-axis) reflect

216   observations (in the y-axis), not *vice versa*[32] (see Methods). Nevertheless, by accurately

217   representing the three dominant factors regulating spring leaf-out, our simple empirical model

218   performed as well as the best phenology models.

219   Our simple regression model provides basic parameters that can easily be incorporated

220   into large-scale vegetation models and Earth system models to project future terrestrial

221   vegetation carbon dynamics. More complex phenological models rely on spatially-explicit

222   parameter-optimization algorithms to account for endodormancy release. Capturing the spatial

223   variation across temperate forests would require large amounts of spatially-uniform

224   phenological data to train these models. Such data does not currently exist and would require a

225   huge coordinated sampling effort. In contrast, our regression model offers a highly

226   parsimonious approach, reflecting the main mechanisms triggering spring phenology without

227   the limitations of model overparameterization. The required parameters can be easily calculated

228   and represented within large-scale vegetation models or Earth system models with minimal

229   increases in complexity. As such, this approach can provide projections of increased veracity

230   without inflating structural uncertainty, which remains the main cause of divergence in

231   vegetation model projections of carbon stocks[33]. Our model can thus provide the empirical

232   relationships that are needed to underpin future projections of temperate spring phenology, and

233   its impacts on terrestrial vegetation carbon dynamics.

234

Future projections of spring leaf-out

235

236   To examine how these ecological mechanisms influence future projections of spring

237   leaf-out, we extrapolated the timing of spring leaf-out until 2100 using two future climate

238   scenarios ("CO_2 stabilization" scenario, RCP 4.5 and "business-as-usual", RCP 8.5; Fig. S7).

239   Specifically, for each scenario, we ran statistical extrapolations of future leaf-out dates, based

240   on the seven best-performing phenology models, including our *full model*, and the simple *null*

241   *model* accounting solely for temperature accumulation. For both climate scenarios, the seven

242   best models gave very similar predictions, estimating a ~60% reduction in the phenological

243   response rates to global warming compared to what would be expected if spring warming was

244   the sole driver of leaf-out phenology (i.e. *null model*) [Fig. 4d]. That is, while the *null model*

245   predicted 25-days earlier leaf unfolding by the end of the 21st century under a "business-as-

246   usual" scenario, the *full model* estimated advances of only 11 days. The *full model* projected

247   similar responses for all species, with the exception of *Fagus sylvatica* (Fig. S8). Under a

248   "business-as-usual" scenario, *F. sylvatica* is expected to advance leaf-out dates less than the

249   other species because pronounced chilling and day length constraints (Fig. 2) cause a lower

250   temperature sensitivity (3.0 days/°C) compared to the other study species (Figs. S6 and S9).

251

Quantifying changes in temperate forest productivity

252

253   To comprehend how our leaf-out predictions will affect future projections of NPP, we

254   used a dynamic global vegetation model (LPJ-GUESS). Previously, spring phenology was

255   implemented as a function of degree-days and winter chilling (see *chilling model* in Figs. 3, 4,

256   and 5)[34]. We parameterized the phenology algorithm using the empirically-derived

257   relationships with day-length at spring onset, and the updated estimates of winter chilling.

258   These changes drastically reduced the projected increases in temperate forest productivity over

259   the rest of this century. Specifically, the standard LPJ-GUESS model (including chilling-only)

260   estimates that cumulative temperate forest NPP will increase by a total of 37 Gt carbon as a

261   result of earlier spring onset over the rest of the century. However, the updated model, including

262   the new empirically-derived information about the ecological constraints on spring phenology

263   estimates an increase of only 12 Gt over the same time period (Figure 5). This 25 Gt reduction

264   in NPP of temperate trees over the rest of the century translates to decreases in temperate forest

265   cumulative net biome productivity of 15.5% (Fig. S10).

266

267   **Conclusions**

268   Our big data approach enables us to test the effects of the three main ecological factors –winter

269   chilling, day-length, and spring warming – that regulate the timing of spring leaf emergence in

270   temperate forest trees. A simple statistical model reflecting these interactive ecological drivers

271   performed as well as the best existing phenology models at predicting spring leaf-out over

272   24,650 individual time series, highlighting that these mechanisms are critical for representing

273   future changes in spring leaf-out. Although spring warming is likely to increase over the rest of

274   the century, the reductions in winter chilling and day length are likely to constrain the future

275   advances in spring leaf emergence. Our statistical model reveals unifying parameters that can

276   be used to represent these important phenological mechanisms in larger biogeochemical

277   models. By representing this information into a global dynamic vegetation model, we find that

278   the expected increases in temperate forest NPP over the rest of the century are substantially

279   reduced relative to previous expectations, which could lead to a reduction in NPP of 0.6

280   Gigatons carbon per year at the end of the 21st century. These results have direct implications

281   for future climate projections, highlighting that forest productivity will be increasingly

282   constrained by factors aside from air temperature in the future.

283

284

285

286

Materials and Methods

Data set. *In situ* observations of leaf-out date were obtained from the Pan European Phenology network[26], which provides open-access phenological data for Europe (mainly Germany, Switzerland, and Austria). We selected leaf-out records of 9 common temperate tree species (7 deciduous angiosperms, 1 deciduous conifer, 1 evergreen conifer) at 4,165 sites (see Fig. S1 for site locations). For the seven angiosperms, leaf-out was defined as the date when unfolded leaves, pushed out all the way to the petiole, were visible on the respective individual (BBCH 11, Biologische Bundesanstalt, Bundessortenamt und Chemische Industrie). For the two conifers *Larix decidua* and *Picea abies* leaf-out was defined as the date when the first needles started to separate ("mouse-ear stage"; BBCH 10).

Information on temperature parameters was derived from a gridded climatic data set of daily minimum and maximum temperatures at 0.5º spatial resolution (approximately 50 km)[35]. We additionally tested the CRU/NCAR dataset (https://crudata.uea.ac.uk/cru/data/ncep/) which also contains daily minimum and maximum temperatures at 0.5º spatial resolution and obtained very similar results (R^2 for degree-days extracted from ref[35] vs. CRU/NCAR dataset = 0.94). Future predictions of daily maximum and minimum temperatures, based on two different climate warming scenarios (RCP 4.5 and 8.5) were obtained from ref[35].

Data reporting. No statistical methods were used to predetermine sample size.

Data cleaning. Following ref[29], we removed (i) leaf-out dates that deviated from an individual's median more than 3 times the median absolute deviation (moderately conservative threshold), (ii) leaf-out dates for which the accumulated degree-days deviated from an individual's median degree-days more than 3 times the median absolute deviation, and (iii) individuals, for which the standard deviation of phenological observations across years was higher than 15. This data cleaning removed 10% of the data, resulting in a total of 24,650 time-series and 727,401

313   phenological observations (individuals x years), with a median time-series length of 29 years

314   (minimally 15 years, maximally 63 years).

315   **Environmental parameters.** Accumulated warming to leaf-out was calculated as the growing

316   degree-days (using 5°C as base temperature) from 1 January until the date of leaf unfolding.

317   We also tested a temperature threshold of 0 °C, which produced very similar results. Here, we

318   only report the results using the threshold of 5 °C. To calculate degree-days, we approximated

319   hourly temperature values with a sine curve based on daily maximum (T_{max}) and minimum

320   temperatures (T_{min}) [equation 1], subtracted 5 (base temperature) from each value, then set all

321   values below the base temperature to zero (because negative development is biologically not

322   possible), and finally calculated the mean of all 24 values for each day, weighting day-time

323   values (= time when sun is above the horizon) 3 times more than night-time values. This

324   weighting was done because the effect of day-time temperature on leaf unfolding is ~3 times

325   higher than that of night-time temperature[36,37].

326   Three factors have been suggested to affect the amount of accumulated warming

327   (degree-days) required to leaf-out: i) preceding autumn temperatures[13,14], ii) exposure to winter

328   chilling[8,10,18], and iii) the prevailing day-length when warming occurs[9,22]. We obtained

329   information for all three factors: Chilling sums were calculated as the sum of chilling days from

330   1 October until mean leaf-out at the respective site. Temperature (T_{hour}) at any time of the day

331   ($time_{day}$) was simulated with a sine curve based on daily maximum (T_{max}) and minimum

332   temperatures (T_{min}) using the following equation:

333

334    $$T_{hour} = \frac{(T_{max}-T_{min})}{2} * \sin\left(\frac{\pi}{12} * time_{day} - \frac{\pi}{2}\right) + \frac{(T_{max}+T_{min})}{2} \tag{1}$$

335

336   This allowed us to calculate the daily proportion of chilling, rather than using a simple

337   presence/absence classification based on daily mean temperatures (e.g., ref. [20]). Multiple studies

338   have reported that temperatures slightly above freezing are most effective in satisfying chilling

339   requirements and assume that effective chilling temperatures range between 0 °C and 5 °C[27,29]:

340

341      $Chill_{hour} = 1 \; if \; 0 \leq T \leq 5$ (2)

342

343   where chilling ($Chill_{hour}$) at any given time of the day depends on the temperature (T).

344 We then calculated daily chilling proportions, e.g., a day in which in 75% of the time

345 temperatures are between 0°C and 5 °C translates to 0.75 chilling days.

346   In addition, we calculated winter chilling including all temperatures below or equal to

347 5 °C (e.g., ref [20]):

348

349      $Chill_{hour} = 1 \; if \; T \leq 5$ (3)

350

351   To obtain information on the prevailing day-length at spring onset (the time when

352 substantial warming occurs in spring), for each time series, a specific degree-day threshold

353 (average degree-days at the mean leaf-out date at the respective site) was used as a proxy for

354 spring onset. The date when the respective degree-day value occurred each year was then

355 transferred to a day-length value (DL) as a function of latitude and date[38]:

356

357      $DL = 24 - \dfrac{24}{\pi} cos^{-1} \left[\dfrac{sin\frac{0.8333\pi}{180} + sin\frac{L\pi}{180} sin\,\varphi}{cos\frac{L\pi}{180} * cos\varphi} \right]$ (4)

358

359      $\varphi = sin^{-1}(0.29795 * cos\,\theta)$ (5)

360

361      $\theta = 0.2163108 + 2 * tan^{-1}(0.9671396 * tan(0.00860 * (DOY - 186)))$ (6)

362

363   where *L* is the latitude of the phenological site and DOY is the day of year when the average

364   degree-days to leaf-out at each site were reached. To infer information on autumn temperatures

365   in the year preceding leaf unfolding, we calculated the mean temperatures of the months

366   September and October, September–November, or October and November for each year.

367   For each species and site, we also analysed the relationship between preseason

368   temperature and leaf-out dates (Fig. S9). Preseason temperature was defined as the average

369   temperature during the 60 days prior to the average leaf unfolding date of an individual.

370

371   **Analysis.** To characterize the relative effects of autumn temperature, winter chilling, and day

372   length on warming required to leaf-out, for each time-series we used univariate linear

373   regressions with the accumulated warming required to leaf-out as the dependent variable, and

374   winter chilling, day length, or autumn temperature in each year as the independent variables

375   (Fig. 2). To visualize the correlations for each species, we removed noise that is due to between-

376   site variation using mixed effects models (R-package lme4) [Fig. S2]. We calculated chilling

377   in two ways (equations 2 and 3), and, in all nine species, the effect of chilling on the amount of

378   warming required to leaf-out was significantly higher when choosing the second option (all

379   temperatures $\leq 5°C$ satisfy chilling requirements; Fig. 2b). To remove possible covariate effects

380   of day-length, we also applied partial correlation analyses between winter chilling and spring

381   warming and obtained similar results, i.e., in all nine species, partial correlation coefficients

382   were higher when using all temperatures $\leq 5°C$ to calculate winter chilling. Similarly, we tested

383   which temperature period in autumn best predicts the amount of warming required to leaf-out,

384   and for each time-series, the autumn temperature period that yielded the highest correlation

385   coefficient was chosen for multivariate modelling.

386   We used breakpoint analysis[39], based on the residual sums of squares, to test whether

387   the effect of day length or winter chilling on required accumulated warming is linear or whether

388   the observed response is flattening beyond a threshold. In 70% and 76% of all time-series, a

389   linear model was preferred over a breakpoint model for the effect of day length or winter

390   chilling, respectively, on required accumulated warming. For the 30% and 25% of time series

391   in which a breakpoint was inferred, we investigated whether steeper slopes are preferred with

392   decreasing day length or chilling. For day length, a steeper slope at shorter days was preferred

393   for only 15% of pixels, while the opposite pattern also was preferred for 15% of pixels. For

394   chilling, a steeper slope under low chilling was only inferred for 13% of pixels, while the

395   opposite pattern was inferred for 11%. We thus rejected the hypothesis that the effect of day

396   length or winter chilling on the amount of warming required to leaf-out is non-linear, i.e.,

397   increases with decreasing day length or chilling.

398   After we had chosen the best autumn period and chilling model for each species, we

399   modelled individual warming requirements using multivariate linear models. Sixteen models

400   were tested against each other (Fig. S3a). The models always included winter chilling and day-

401   length as fixed effects. Additionally, we either included or excluded autumn temperatures as

402   explanatory variable. We also tested for an interaction term between day-length and winter

403   chilling, because day-length and chilling cues can interact, with long days substituting for

404   insufficient chilling and *vice versa*[21,22]. We also tested models including chilling and day length

405   as exponential terms (which did not affect model precision and projections; Figs. S5 and S6).

406   In addition to our multivariate model (hereafter referred to as *full model*), we applied a *chilling*

407   *model*, in which the amount of warming required to leaf-out is solely affected by winter chilling

408   (equation 7), and a *degree-day model*, in which leaf-out is solely driven by degree-day

409   accumulation. The starting date of degree-day accumulation was fixed to 1 January. All models

410   were fitted separately to individuals, because we were interested in temporal patterns within

411   individuals (rather than spatial patterns among individuals), and spring warming, day-length,

412   and chilling requirements differ among individuals[40].

413

414

415   *Process-based phenological models*

416   We ran 17 parameterized process-based phenological models from the literature to test the

417   overall performance of our *full model* against existing models. We used the R-package

418   PHENOR[41] to calibrate the models. Model parameters were optimized using the GenSA

419   algorithm[42], combining both the Boltzmann machine and faster Cauchy machine simulated

420   annealing approaches for fast optimizations[43]. According to ref[41], the number of iterations was

421   set to 40,000 with a starting temperature of 10,000.

422

423   *Model evaluation*

424   To judge the performance of phenological models, previous studies relied either solely on root-

425   mean square errors of observed vs predicted leaf-out dates[12,44,45] or additionally evaluated

426   model predictions by comparing predicted (in the y-axis) vs observed (in the x-axis) leaf-out

427   dates[41,46,47]. However, such regression to evaluate models is incorrect, leading to erroneous

428   estimates of the slope and intercept[32]. Especially in directional models such as spring

429   phenological projections, where future climate conditions will lead to ever earlier occurrence

430   dates, models need to be evaluated by analyzing intercept and slope components of observed

431   (in the y-axis) vs predicted dates (in the x-axis). To do so, we conducted Wald-test based

432   comparisons[48] using the linearHypothesis function in the R-package car, allowing us to test for

433   each individual site whether the slopes and intercepts of observed *vs.* predicted leaf-out dates

434   differ significantly from 1 and 0, respectively (Fig. 4a,b). For each species, we also obtained

435   the overall model fit (R^2 values) and RMSE errors for observed *versus* predicted values (Figs.

436   3c, 4c, and S4). Next, we applied 10-fold cross-validations[49], and tested whether projected leaf-

437   out dates capture (i) observed temporal trends and (ii) the observed sensitivity of leaf-out dates

438   to spring temperatures (Figs. 3a,b, S5, and S6). To calculate temperature sensitivity trends

439   based on time-series, we had to remove noise that is due to between-site variation. This was

440 done by adjusting the data using mixed effects modelling available through the R-package

441 lme4.

442

Future projections of spring onset

444 To forecast leaf-out dates based on our models, we used future projections of daily minimum

445 and maximum temperatures from two climate scenarios (Fig. S7)[35]. Emissions in the RCP 4.5

446 climate scenario peak around 2040 and then decline. In the RCP 8.5 climate scenario emissions

447 continue to rise throughout the 21st century.

448

Land-surface flux projections

450 We used LPJ-GUESS, a dynamic global vegetation model[50], to simulate the effects of shifting

451 spring phenology on temperate forest carbon balances (net primary productivity [NPP] and net

452 biome productivity). LPJ-GUESS represents vegetation growth and dynamics using a mixture

453 of plant functional types that respond to forcing from the climate (temperature, precipitation,

454 incoming shortwave radiation), atmospheric CO_2 mixing ratios and soil type. The successional

455 structure of vegetation is simulated using multiple (here ten) replicate patches in each grid cell,

456 which are subject to stochastic processes of establishment and mortality. Photosynthesis,

457 respiration, stomatal conductance and phenology in LPJ-GUESS are simulated on a daily time

458 step.

459   Limitations in availability of the necessary driving data and requirements for

460 parsimony to operate at large-scales mean that common process-based phenological models

461 cannot easily be incorporated into global vegetation models such as LPJ-GUESS. Instead, in

462 common with most other such models (e.g. refs[51,52]), spring phenology was represented by an

463 exponential relationship between growing degree-days to leaf-out and the length of the chilling

464 period (*chilling model*). In LPJ-GUESS the relationship was formulated as follows[34]:

465

466     $GDD° = \alpha + \beta e^{-\kappa C}$ (7)

467

468   where C is the length of the chilling period and α, β, and κ are constants specific to plant

469   functional types.

470

471   Based on our empirical findings we replaced this equation by the following (*full model*):

472

473     $GDD° = \alpha + \beta C + \gamma D + \delta CD$ (8)

474

475   where C is the length of the chilling period, D is the day length at spring onset, CD is the

476   interaction between chilling and day length, and α, β, γ, and δ are coefficients specific to plant

477   functional types. The length of the chilling period was defined as the number of days <5°C from

478   1 October, day length at spring onset was defined relative to a degree-day threshold (see table

479   1). We calculated a specific spring onset for each functional type because, the needleleaf

480   summergreen species *Larix decidua*, for example, flushes earlier than many broadleaf

481   summergreen trees. Three functional types of trees (BSI, broadleaved summergreen shade-

482   intolerant; BST, broadleaved summergreen shade-tolerant; NS, needleleaved summergreen)

483   were present in our species sampling. Following ref[53], *Fagus sylvatica* and *Tilia cordata* were

484   treated as shade tolerant, *Aesculus hippocastanum*, Alnus glutinosa, *Betula pendula*, *Fraxinus*

485   *excelsior*, and *Quercus robur* as shade intolerant. Leaf-out phenology of *Picea abies* was not

486   included in LPJ-GUESS because, in evergreen species, onset of photosynthetic activity in

487   spring is not dependent on the flushing of new buds. In addition to the deciduous plant

488   functional types described above, LPJ-GUESS simulations also included a temperate

489   needleleaved evergreen tree, a boreal needleleaved evergreen shade-tolerant tree, a boreal

490   needleleaved evergreen shade-intolerant tree and a C3 grass[50], with the distributions of each

491   functional type governed by model-internal processes of competition. All simulations were run

492   as potential natural vegetation (i.e. without land management) and the outputs were masked and

493   rescaled to current temperate forest area as defined by Hansen et al.[54].

494   Daily climate forcing data came from the r1i1p1 ensemble member of the IPSL-

495   CM5A-LR model from CMIP5[55] for 1850-2099 following the RCP 8.5 scenario, bias-corrected

496   to 1960-1999 WATCH climate[56], as prepared for the ISI-MIP2 project. Atmospheric CO_2

497   mixing ratios were as prescribed for the RCP 8.5 scenario of CMIP5 and N deposition data was

498   taken from Lamarque et al.[57]. Simulations were spun-up for 500 years using recycled, detrended

499   1850-1879 climate, and 1850 atmospheric CO_2 mixing ratio and N deposition. They were then

500   run under fully transient environmental forcings from 1850-2099. The spatial resolution was

501   0.5° x 0.5°. In total four simulations were conducted: simulations with the original and updated

502   phenology algorithms, and two further simulations in which, for each of the algorithms, leaf

503   out dates from 2010 onwards were forced by mean 2001-2010 daily temperatures in each grid

504   cell, so as to provide a baseline from which to identify the effects of the phenology algorithm

505   on the carbon cycle.

506

507   **References**

508   1.   Keenan, T. F. *et al.* Net carbon uptake has increased through warming-induced changes

509   in temperate forest phenology. *Nat. Clim. Chang.* **4**, 598–604 (2014).

510   2.   Richardson, A. D. *et al.* Climate change, phenology, and phenological control of

511   vegetation feedbacks to the climate system. *Agric. For. Meteorol.* **169**, 156–173 (2013).

512   3.   Richardson, A. D. *et al.* Influence of spring and autumn phenological transitions on forest

513   ecosystem productivity. *Philos. Trans. R. Soc. B Biol. Sci.* **365**, 3227–3246 (2010).

514   4.   Chuine, I. Why does phenology drive species distribution? *Philos. Trans. R. Soc. B Biol.*

515   *Sci.* **365**, 3149–3160 (2010).

516   5.   Menzel, A. & Fabian, P. Growing season extended in Europe. *Nature* **397**, 659 (1999).

517   6.   Zohner, C. M. & Renner, S. S. Common garden comparison of the leaf-out phenology

518   of woody species from different native climates, combined with herbarium records,

519   forecasts long-term change. *Ecol. Lett.* **17**, 1016–1025 (2014).

520 7. Cook, B. I. *et al.* Sensitivity of Spring Phenology to Warming Across Temporal and

521   Spatial Climate Gradients in Two Independent Databases. *Ecosystems* **15**, 1283–1294

522   (2012).

523 8. Zohner, C. M., Benito, B. M., Fridley, J. D., Svenning, J. C. & Renner, S. S. Spring

524   predictability explains different leaf-out strategies in the woody floras of North America,

525   Europe and East Asia. *Ecol. Lett.* **20**, 452–460 (2017).

526 9. Zohner, C. M., Benito, B. M., Svenning, J. C. & Renner, S. S. Day length unlikely to

527   constrain climate-driven shifts in leaf-out times of northern woody plants. *Nat. Clim.*

528   *Chang.* **6**, 1120–1123 (2016).

529 10. Laube, J. *et al.* Chilling outweighs photoperiod in preventing precocious spring

530   development. *Glob. Chang. Biol.* **20**, 170–182 (2014).

531 11. Polgar, C., Gallinat, A. & Primack, R. B. Drivers of leaf-out phenology and their

532   implications for species invasions: Insights from Thoreau's Concord. *New Phytol.* **202**,

533   106–115 (2014).

534 12. Basler, D. Evaluating phenological models for the prediction of leaf-out dates in six

535   temperate tree species across central Europe. *Agric. For. Meteorol.* **217**, 10–21 (2016).

536 13. Fu, Y. S. H. *et al.* Variation in leaf flushing date influences autumnal senescence and

537   next year's flushing date in two temperate tree species. *Proc. Natl. Acad. Sci.* **111**, 7355–

538   7360 (2014).

539 14. Heide, O. M. High autumn temperature delays spring bud burst in boreal trees,

540   counterbalancing the effect of climatic warming. *Tree Physiol.* **23**, 931–936 (2003).

541 15. Luedeling, E., Girvetz, E. H., Semenov, M. A. & Brown, P. H. Climate change affects

542   winter chill for temperate fruit and nut trees. *PLoS One* **6**, (2011).

543 16. Yu, H., Luedeling, E. & Xu, J. Winter and spring warming result in delayed spring

544   phenology on the Tibetan Plateau. *Proc. Natl. Acad. Sci.* **107**, 22151–22156 (2010).

545   17.   Heide, O. M. Dormancy release in beech buds (Fagus sylvatica) requires both chilling

546   and long days. *Physiol. Plant.* **89**, 187–191 (1993).

547   18.   Heide, O. M. Daylength and thermal time responsese of budburst during dormancy

548   release in some northern deciduous trees. *Physiol. Plant.* **88**, 531–540 (1993).

549   19.   Körner, C. & Basler, D. Phenology under global warming. *Science (80-.).* **327**, 1461–

550   1462 (2010).

551   20.   Fu, Y. H. *et al.* Declining global warming effects on the phenology of spring leaf

552   unfolding. *Nature* **526**, 104 (2015).

553   21.   Vitasse, Y. & Basler, D. What role for photoperiod in the bud burst phenology of

554   European beech. *Eur. J. For. Res.* **132**, 1–8 (2013).

555   22.   Zohner, C. M. & Renner, S. S. Perception of photoperiod in individual buds of mature

556   trees regulates leaf-out. *New Phytol.* **208**, 1023–1030 (2015).

557   23.   Fu, Y. H. *et al.* Daylength helps temperate deciduous trees to leaf-out at the optimal time.

558   *Glob. Chang. Biol.* **25**, 2410–2418 (2019).

559   24.   Vitasse, Y. Ontogenic changes rather than difference in temperature cause understory

560   trees to leaf out earlier. *New Phytol.* **198**, 149–155 (2013).

561   25.   Chen, M., Melaas, E. K., Gray, J. M., Friedl, M. A. & Richardson, A. D. A new seasonal-

562   deciduous spring phenology submodel in the Community Land Model 4.5: impacts on

563   carbon and water cycling under future climate scenarios. *Glob. Chang. Biol.* **22**, 3675–

564   3688 (2016).

565   26.   Templ, B. *et al.* Pan European Phenological database (PEP725): a single point of access

566   for European data. *Int. J. Biometeorol.* **62**, 1109–1113 (2018).

567   27.   Coville, F. V. The influence of cold in stimulating the growth of plants. *Proc. Natl. Acad.*

568   *Sci.* **6**, 151–160 (1920).

569   28.   Hunter, A. F. & Lechowicz, M. J. Predicting the timing of budburst in temperate trees.

570   *J. Appl. Ecol.* **29**, 597–604 (1992).

571   29.   Vitasse, Y., Signarbieux, C. & Fu, Y. H. Global warming leads to more uniform spring

572   phenology across elevations. *Proc. Natl. Acad. Sci.* 201717342 (2017).

573   doi:10.1073/pnas.1717342115

574   30.   Fu, Y. H. *et al.* Daylength helps temperate deciduous trees to leaf-out at the optimal time.

575   *Glob. Chang. Biol.* gcb.14633 (2019). doi:10.1111/gcb.14633

576   31.   Brelsford, C. C. & Robson, T. M. Blue light advances bud burst in branches of three

577   deciduous tree species under short-day conditions. *Trees - Struct. Funct.* 1–8 (2018).

578   doi:10.1007/s00468-018-1684-1

579   32.   Piñeiro, G., Perelman, S., Guerschman, J. P. & Paruelo, J. M. How to evaluate models:

580   Observed vs. predicted or predicted vs. observed? *Ecol. Modell.* **216**, 316–322 (2008).

581   33.   Nishina, K. *et al.* Decomposing uncertainties in the future terrestrial carbon budget

582   associated with emission scenarios, climate projections, and ecosystem simulations

583   using the ISI-MIP results. *Earth Syst. Dyn.* **6**, 435–445 (2015).

584   34.   Sykes, M. T., Prentice, I. C. & Cramer, W. A Bioclimatic Model for the Potential

585   Distributions of North European Tree Species Under Present and Future Climates. **23**,

586   203–233 (1996).

587   35.   Beer, C. *et al.* Harmonized European Long-Term Climate Data for Assessing the Effect

588   of Changing Temporal Variability on Land–Atmosphere CO_2 Fluxes*. *J. Clim.* **27**,

589   4815–4834 (2014).

590   36.   Piao, S. *et al.* Leaf onset in the northern hemisphere triggered by daytime temperature.

591   *Nat. Commun.* **6**, (2015).

592   37.   Fu, Y. H. *et al.* Three times greater weight of daytime than of night-time temperature on

593   leaf unfolding phenology in temperate trees. *New Phytol.* **212**, 590–597 (2016).

594   38.   Forsythe, W. C., Rykiel, E. J., Stahl, R. S., Wu, H. i. & Schoolfield, R. M. A model

595   comparison for daylength as a function of latitude and day of year. *Ecol. Modell.* **80**, 87–

596   95 (1995).

597   39.   Richardson, A. D. *et al.* Ecosystem warming extends vegetation activity but heightens

598   vulnerability to cold temperatures. *Nature* **560**, 368–371 (2018).

599   40.   Zohner, C. M., Mo, L. & Renner, S. S. Global warming reduces leaf-out and flowering

600   synchrony among individuals. *Elife* (2018).

601   41.   Hufkens, K., Basler, D., Milliman, T., Melaas, E. K. & Richardson, A. D. An integrated

602   phenology modelling framework in r. *Methods Ecol. Evol.* **9**, 1276–1285 (2018).

603   42.   Xiang, Y., Gubian, S., Suomela, B. & Hoeng, J. Generalized simulated annealing for

604   global optimization: the GenSA Package. *R J.* **5**, 13–28 (2013).

605   43.   Tsallis, C. & Stariolo, D. A. Generalized simulated annealing. *Phys. A Stat. Mech. its*

606   *Appl.* **233**, 395–406 (1996).

607   44.   Vitasse, Y., Schneider, L., Rixen, C., Christen, D. & Rebetez, M. Increase in the risk of

608   exposure of forest and fruit trees to spring frosts at higher elevations in Switzerland over

609   the last four decades. *Agric. For. Meteorol.* **248**, 60–69 (2018).

610   45.   Fu, Y. H., Campioli, M., Van Oijen, M., Deckmyn, G. & Janssens, I. A. Bayesian

611   comparison of six different temperature-based budburst models for four temperate tree

612   species. *Ecol. Modell.* **230**, 92–100 (2012).

613   46.   Schaber, J. & Badeck, F. W. Physiology-based phenology models for forest tree species

614   in Germany. *Int. J. Biometeorol.* **47**, 193–201 (2003).

615   47.   Delpierre, N. *et al.* Modelling interannual and spatial variability of leaf senescence for

616   three deciduous tree species in France. *Agric. For. Meteorol.* **149**, 938–948 (2009).

617   48.   Fox, J. *Applied Regression Analysis and Generalized Linear Models.* (SAGE

618   Publications, Inc, 2016).

619   49.   M. Stone. Cross-Validatory Choice and Assessment of Statistical Predictions. *Proc. R.*

620   *Soc. B Biol. Sci.* **36**, 111–174 (1974).

621   50.   Smith, B. *et al.* Implications of incorporating N cycling and N limitations on primary

622   production in an individual-based dynamic vegetation model. *Biogeosciences* **11**, 2027–

623   2054 (2014).

624   51. Clark, D. B. *et al.* The Joint UK Land Environment Simulator (JULES), model

625   description – Part 2: Carbon fluxes and vegetation dynamics. *Geosci. Model Dev.* **4**, 701–

626   722 (2011).

627   52. Krinner, G. *et al.* A dynamic global vegetation model for studies of the coupled

628   atmosphere-biosphere system. *Global Biogeochem. Cycles* **19**, 1–33 (2005).

629   53. Niinemets, Ü. & Valladares, F. Tolerance to shade, drought, and waterlogging of

630   temperate Northern Hemisphere trees and shrubs. *Ecol. Monogr.* **76**, 521–547 (2006).

631   54. Hansen, M. C. *et al.* High-Resolution Global Maps of 21st-Century Forest Cover

632   Change. *Science (80-.).* **850**, 2011–2014 (2013).

633   55. Taylor, K. E., Stouffer, R. J. & Meehl, G. A. An overview of CMIP5 and the experiment

634   design. *Bull. Am. Meteorol. Soc.* **93**, 485–498 (2012).

635   56. Hempel, S., Frieler, K., Warszawski, L., Schewe, J. & Piontek, F. A trend-preserving

636   bias correction – The ISI-MIP approach. *Earth Syst. Dyn.* **4**, 219–236 (2013).

637   57. Lamarque, J. F. *et al.* Multi-model mean nitrogen and sulfur deposition from the

638   atmospheric chemistry and climate model intercomparison project (ACCMIP):

639   Evaluation of historical and projected future changes. *Atmos. Chem. Phys.* **13**, 7997–

640   8018 (2013).

641

642

643

644

645

646

647

Competing interest declaration

The authors declare that there are no competing interests.

677 **Table 1 | Coefficients estimated for the full model according to equation 8.** Separate

678 coefficients were obtained for each plant functional type and reflect the average across species

679 and sites. Spring onset refers to the average degree-days used to calculate day-length. Species

680 used to infer functional-type specific coefficients: broadleaved summergreen shade-intolerant

681 = *Aesculus hippocastanum, Alnus glutinosa, Betula pendula, Fraxinus excelsior,* and *Quercus*

682 *robur*; broadleaved summergreen shade-tolerant = *Fagus sylvatica* and *Tilia cordata*;

683 needleleaf summergreen = *Larix decidua*.

684

Functional type	α	β	γ	δ	Spring onset (GDD)
Temperate broadleaf summergreen shade-intolerant (BSI)	730.64	-0.05	-34.78	-0.01	215
Temperate broadleaf summergreen shade-tolerant (BST)	1008.88	-1.16	-53.46	0.06	220
Boreal needleleaf summergreen (NS)	618.18	-2.49	-33.50	0.15	150

685

686

687

688

689

690

691
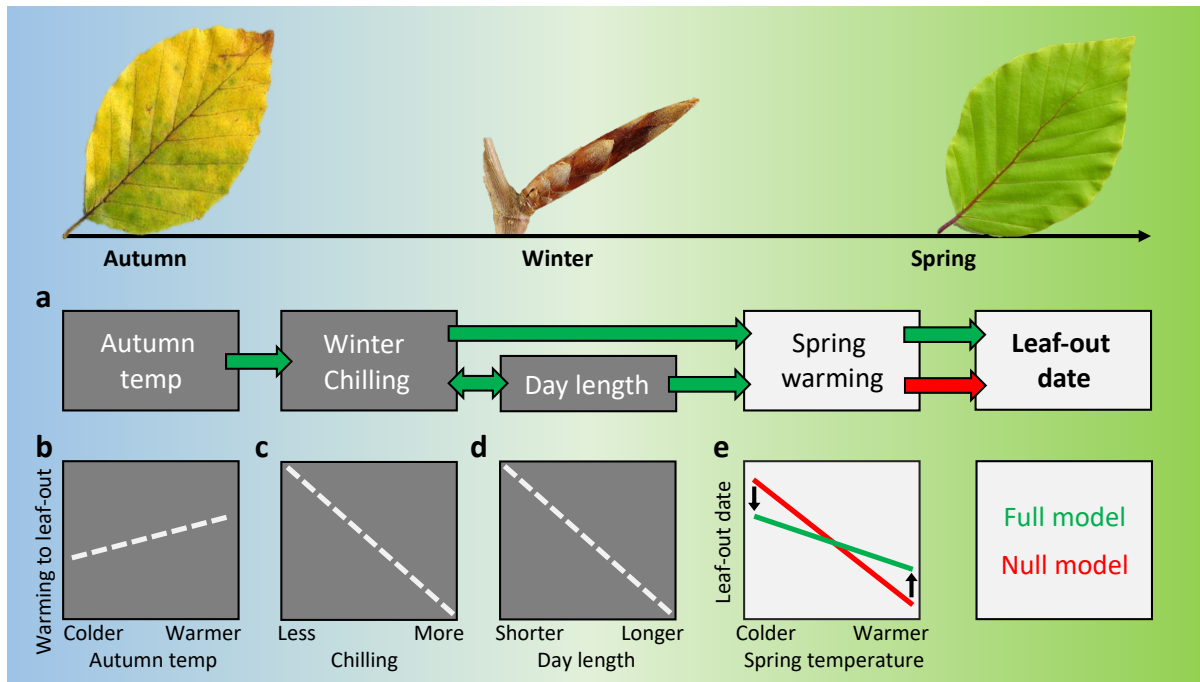
Figure 1 | Testing for interactive climate effects on the timing of spring leaf-out. a, In the *full model* (green), the amount of warming required to leaf-out is directly affected by winter chilling and spring day length, winter chilling interacts with day-length, and autumn temperatures affect winter chilling. In the *Null model* (red), leaf-out is solely driven by spring warming. **b–d,** The interactive effects among climate factors should cause warming requirements to increase under warmer autumns (**b**), reduced chilling (**c**), or shorter day length (**d**). **e**, Under cold spring conditions, leaf-out should occur earlier than expected from the *Null model* because long days and long chilling reduce the amount of warming required to leaf-out; under warm spring conditions, leaf-out should occur later than expected from the *Null model* because short days and short chilling increase the amount of warming required to leaf-out.
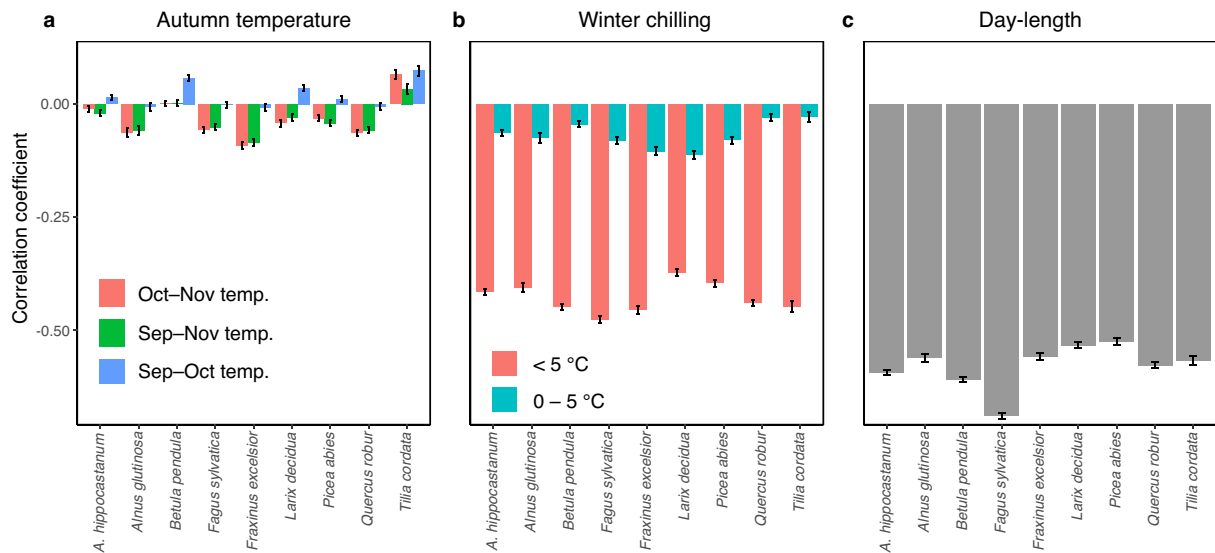
Figure 2 | The effects of autumn temperature (a), winter chilling (b), and day-length (c) on accumulated warming required to leaf-out. Pearson correlation coefficients (± 2 standard errors) are shown for each parameter. **a**, The mean temperatures of the months October and November, September to November, or September and October were used to calculate autumn temperatures. **b**, Two different temperature ranges were used to calculate winter chilling: all temperatures below 5°C (red) or temperatures between 0°C and 5°C (turquoise). **c**, The relationship between day-length at spring onset and accumulated warming required to leaf-out. Number of analysed time-series per species: *Aesculus hippocastanum*, 3703; *Alnus glutinosa*, 1841; *Betula pendula*, 3663; *Fagus sylvatica,* 3091; *Fraxinus excelsior*, 2178; *Larix decidua*, 2644; *Picea abies*, 2942; *Quercus robur*, 3152; *Tilia cordata*, 1436.
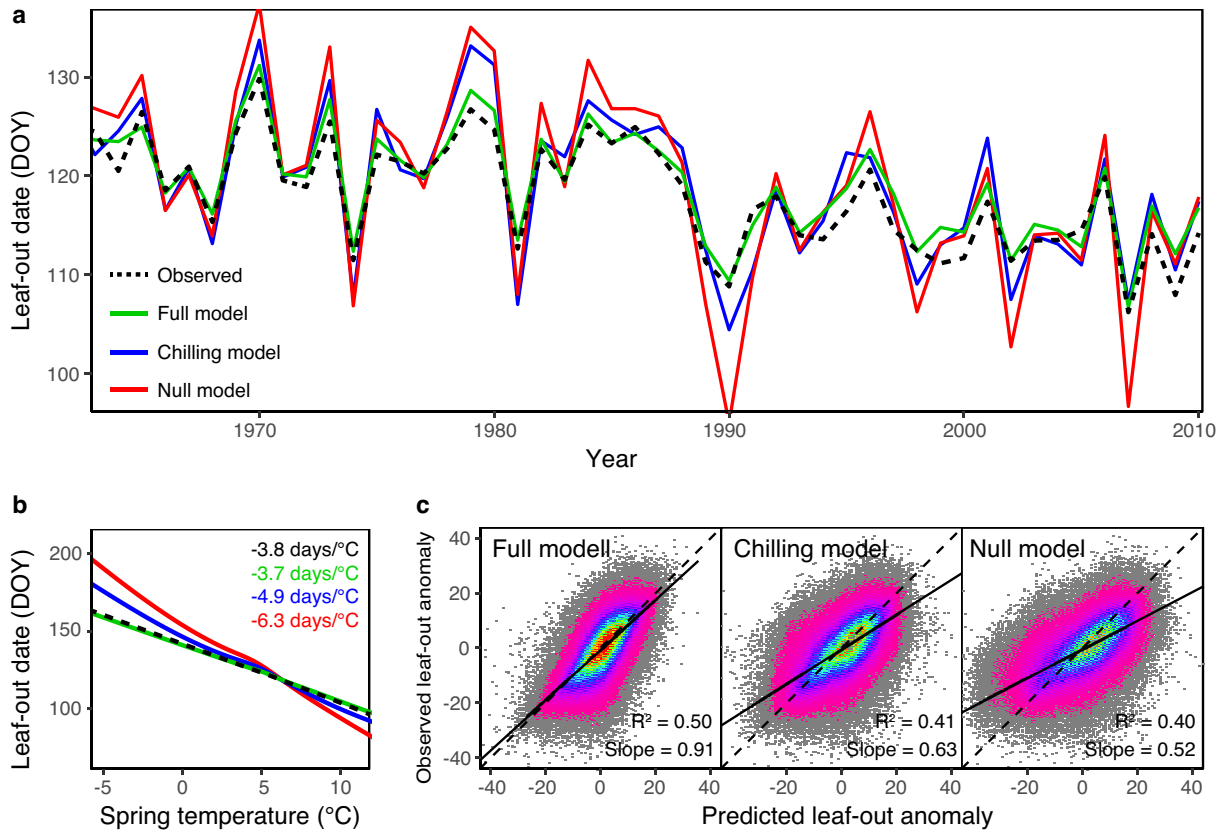
Figure 3 | Leaf-out date predictions based on the empirical relationships between required accumulated warming and autumn temperature, winter chilling, and day-length (see Figure 1). a, b, Observed and empirically modelled leaf-out dates using 10-fold cross-validations in response to year (**a**) and spring temperature (**b**) averaged across all nine study species (observed leaf-out = black lines; *full model* = green lines; *chilling model* = blue lines; *Null model* = red lines). See Figs. S5 and S6 for species-specific plots. Loess smoothing curves in b) are based on random-effects models to control for differences among sites. **c**, Observed versus predicted leaf-out dates of the *full model*, the *chilling model*, and the *Null model*. Solid lines show linear regression fit, dashed lines show the 1:1 line. For the *chilling model* and the *Null model*, the intercept differed significantly from 0 and the slope differed from 1 ($P < 0.05$). To standardize among sites, observed and predicted leaf-out dates are shown as anomalies, i.e., as deviation from the mean observed leaf-out date at each site.
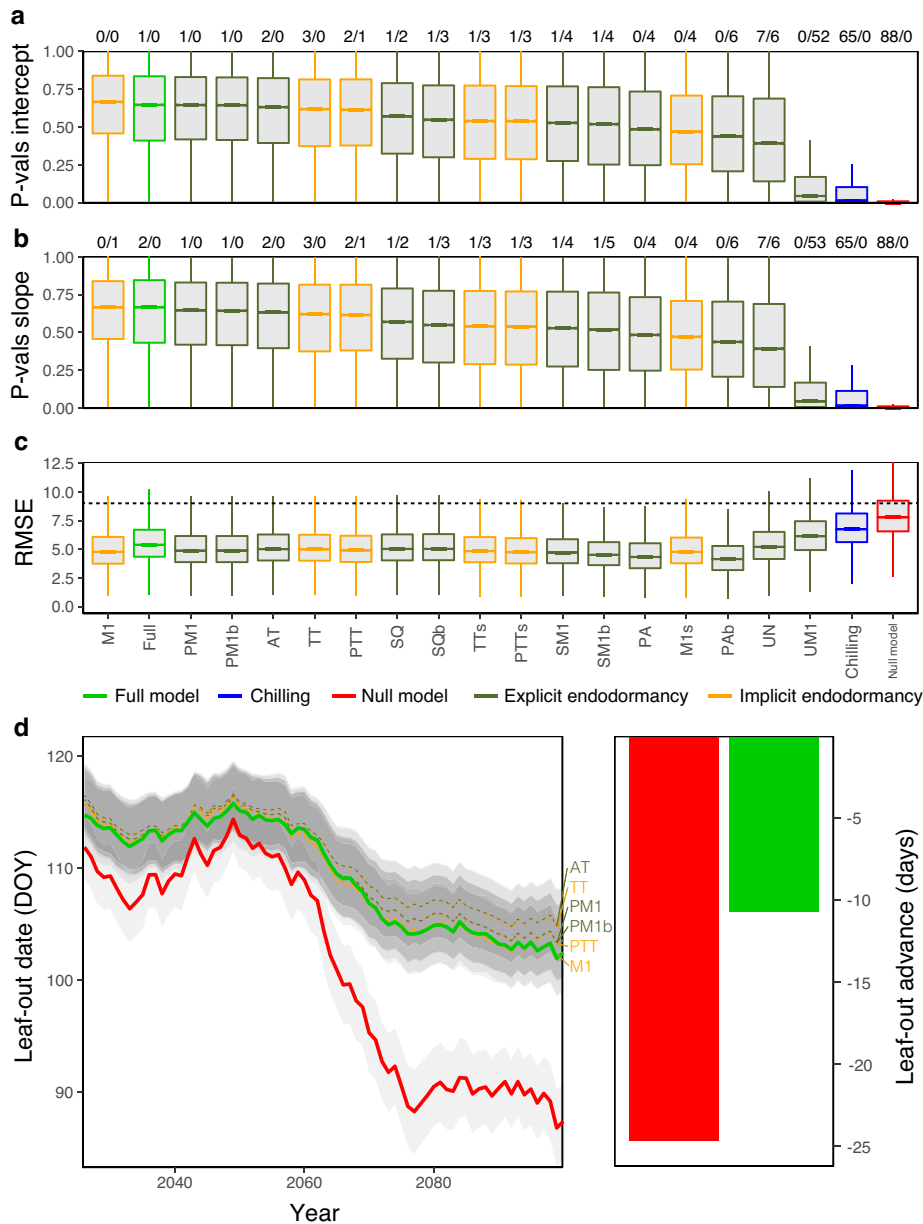
Figure 4 | Model evaluation and future projections of Central European leaf-out dates. a-c, Model comparison of the three empirical models applied in this study (green = *full model*, blue = *chilling model*, red = *Null model*) and 17 process-based models from the literature. **a**, Significance values reporting whether the slope of observed versus predicted leaf-out dates differs from 1. Numbers above indicate the percentages of sites for which the model slopes were significantly ($P<0.05$) smaller (= overprediction) or larger than 1 (= underprediction). **b**, Significance values reporting whether the intercept of observed versus predicted leaf-out dates differs from 0. Numbers above indicate the percentages of sites for which the model intercepts were significantly larger (= overprediction) or smaller than 0 (= underprediction). **c**, Root-mean-square errors of models. The dashed line shows the average RMSE expected under a Null-model where leaf-out dates do not differ among years. **d**, Future leaf-out projections (15-year moving averages for nine species) under the RCP 8.5 climate-scenario, based on the seven best performing models and the *Null model*. The grey area indicates one s.e. either side of the mean. Right panel shows estimated advances in leaf-out by the end of the 21st century (2080–2100) compared to the average leaf-out dates between 1990–2010 according to the *full model* (green) and the *Null model* (red).
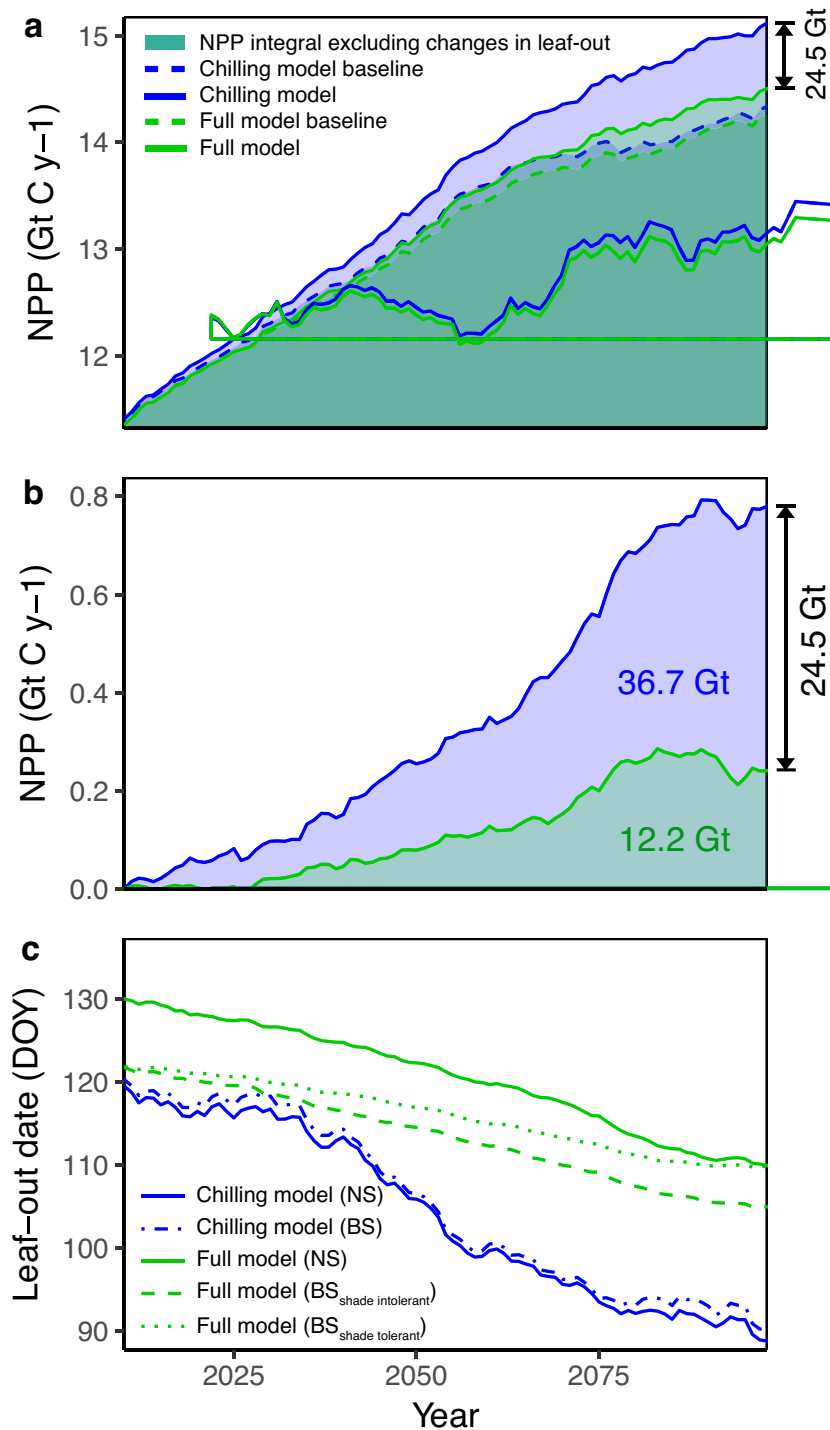
Figure 5 | Effects of leaf-out changes in Northern Hemisphere temperate forests on net primary productivity (NPP). a, Annual forest NPP (above 23°N latitude) over the 21st century, simulating spring leaf-out times with the *chilling model* (solid blue line) or the *full model* (solid green line). Dashed lines show the baselines assuming no leaf-out changes in the future (phenology fixed at years 2001-2010). **b,** Increases in NPP that are solely caused by leaf-out shifts simualted with the *chilling model* and the *full model*. Arrows in a) and b) show the cumulative difference in NPP between the standard LPJ-GUESS model (including the *chilling model*) and the updated model (including our *full model*). **c,** Differences in average leaf-out times of Northern Hemisphere temperate forests simualted with the *chilling model* and the *full model*. Plant functional types: NS, needleleaved summergeen; BS, broadleaved summergreen (either shade tolerant or intolerant).

Supplementary data

Interactive climate factors restrict future increases in spring tree productivity

Authors: Constantin M. Zohner*[1], Lidong Mo[1], Thomas A.M. Pugh[2,3], Jean-Francois Bastin[1], and Thomas W. Crowther[1]

Affiliations:

[1]Institute of Integrative Biology, ETH Zurich (Swiss Federal Institute of Technology), Universitätsstrasse 16, 8092 Zurich, Switzerland

[2]School of Geography, Earth and Environmental Sciences, University of Birmingham, Edgbaston, Birmingham, B15 2TT, UK

[3]Birmingham Institute of Forest Research, University of Birmingham, Edgbaston, Birmingham, B15 2TT, UK

List of supplementary contents

824
825
826 **Figure S1 | Locations of the 4,165 sites used in this study.** Each site contains long-term leaf-
827 out observations (>15 years) for at least one species. On average, information on six species
828 was available per site.

829

830
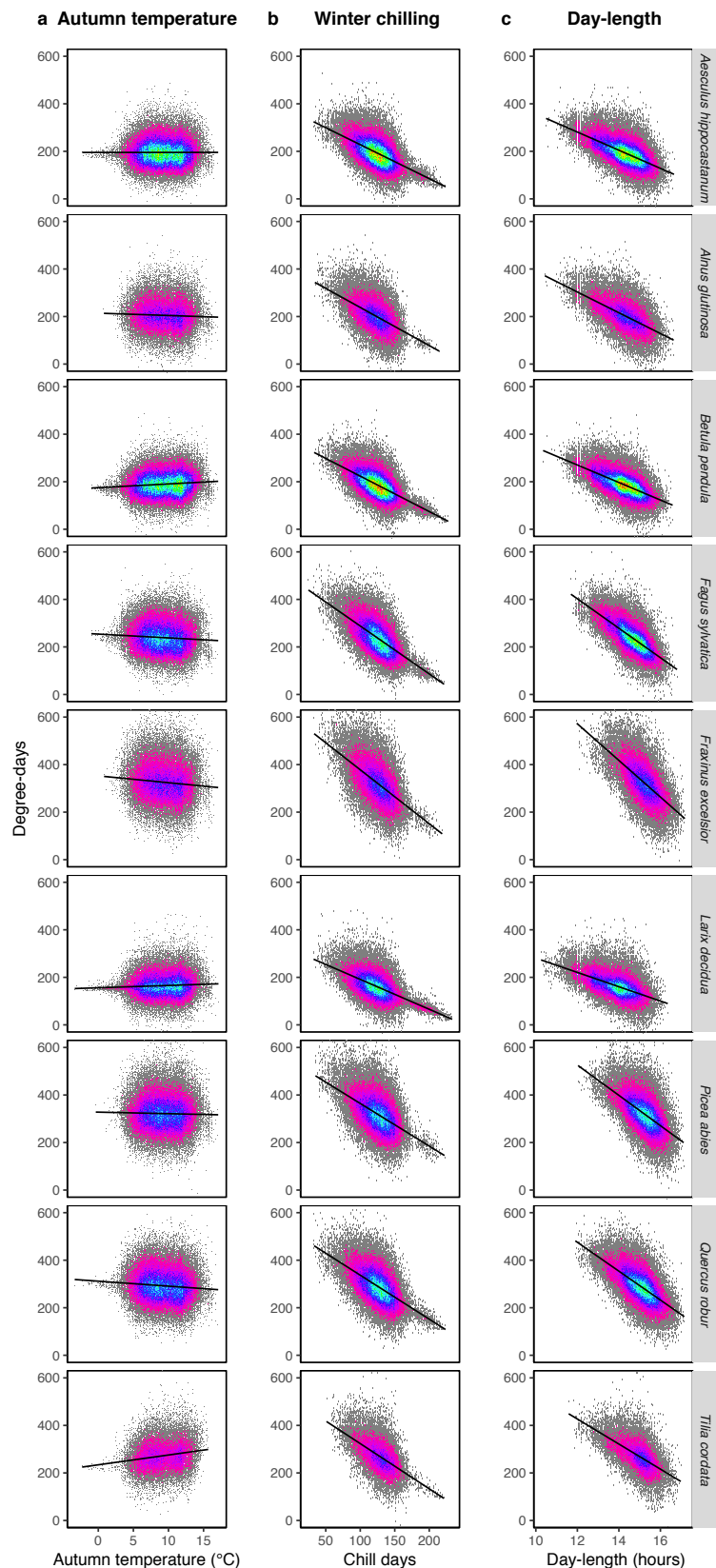
831 **Figure S2 | The univariate effects of autumn temperature (a), winter chilling (b), and day-**

832 **length (c) on accumulated warming (degree-days) required to leaf-out.** Random effects

833 models were applied to remove site effects for each species. Winter chilling was calculated

834 using all temperatures below 5 °C (see Methods).

835
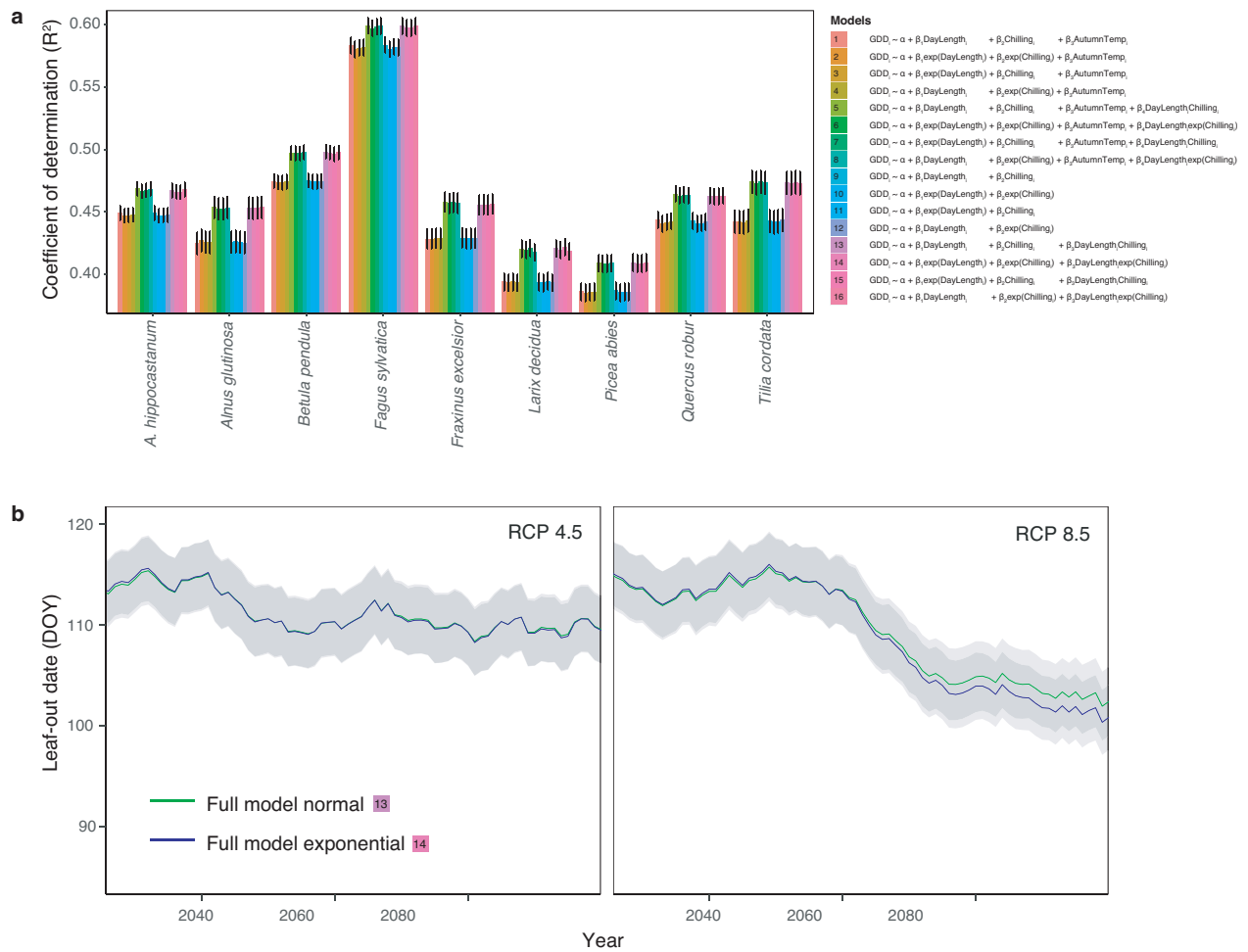
Figure S3 | Comparison of empirical model equations. a, Comparison of 16 models testing the relationships between accumulated warming required to leaf-out and day-length, winter chilling, and autumn temperatures in the nine study species. Model equations are shown on the right. Across all species, models including an interaction term between day-length and winter chilling had significantly higher R^2 values. Whether autumn temperature was included as a fixed effect or not did not affect the model fit. Also, model fit was unaffected by whether day-length and winter chilling were included as exponential terms or not. **b**, Future projections of Central European leaf-out dates including winter chilling and day length as normal (green lines) or exponential terms (blue lines) in the model (equations 13 and 14 in panel a). 15-year moving averages for nine species are shown. Left panel: 'CO$_2$ stabilization' climate scenario (RCP 4.5); Right panel: 'business-as-usual' scenario (RCP 8.5). The grey area indicates one s.e. either side of the mean.
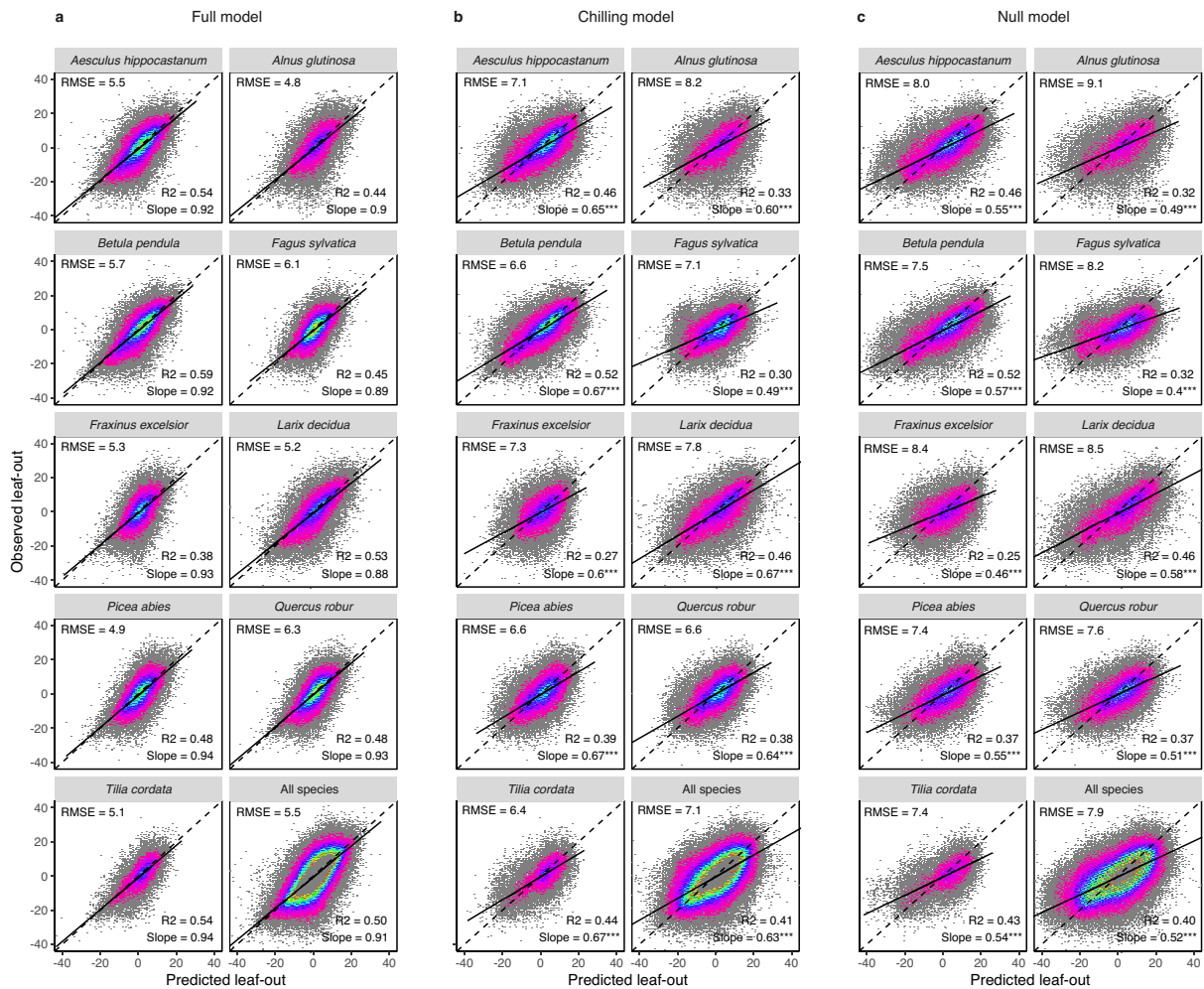
854
855

Figure S4 | Observed versus predicted leaf-out dates of the *full model* (a), the *chilling model* (b), and the *Null model* (c). Solid lines show linear regression fit, dashed lines show the 1:1 line. RMSE values, R^2 values, and regression slopes are shown in each panel, asterisks indicate that the slope differs significantly from 1 (Wald-test; *P <0.05, **P <0.01, ***P <0.001). To standardize among sites, observed and predicted leaf-out dates are shown as anomalies, i.e., as deviation from the mean observed leaf-out date at each site.

862
863
864
865
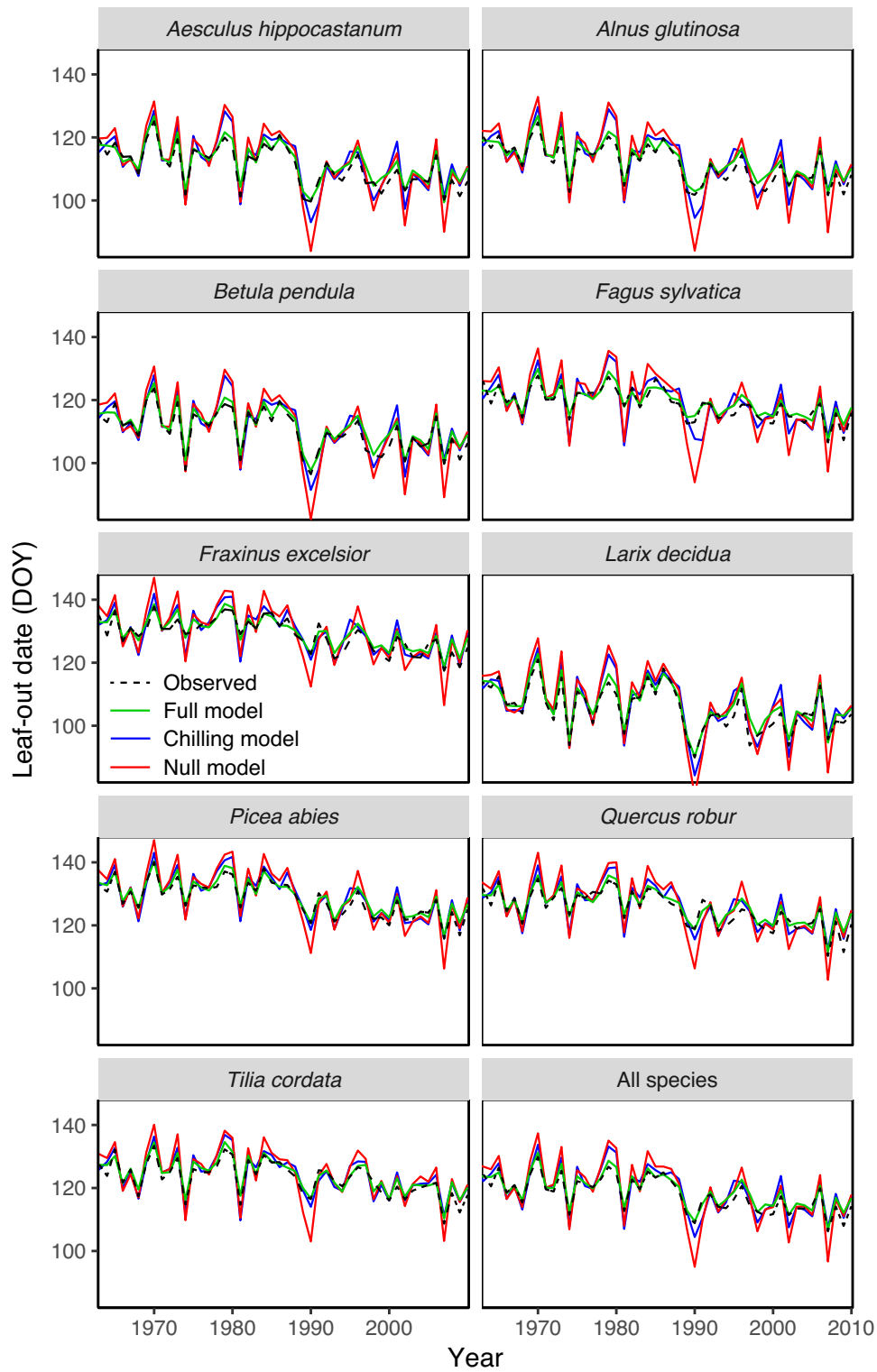
866
867
Figure S5 | Temporal projections of leaf-out dates of the nine study species. Observed
(black lines) and empirically modelled average leaf-out dates using 10-fold cross-validations in
response to year (*full model* = green lines; *chilling model* = blue lines; *Null model* = red lines).
871
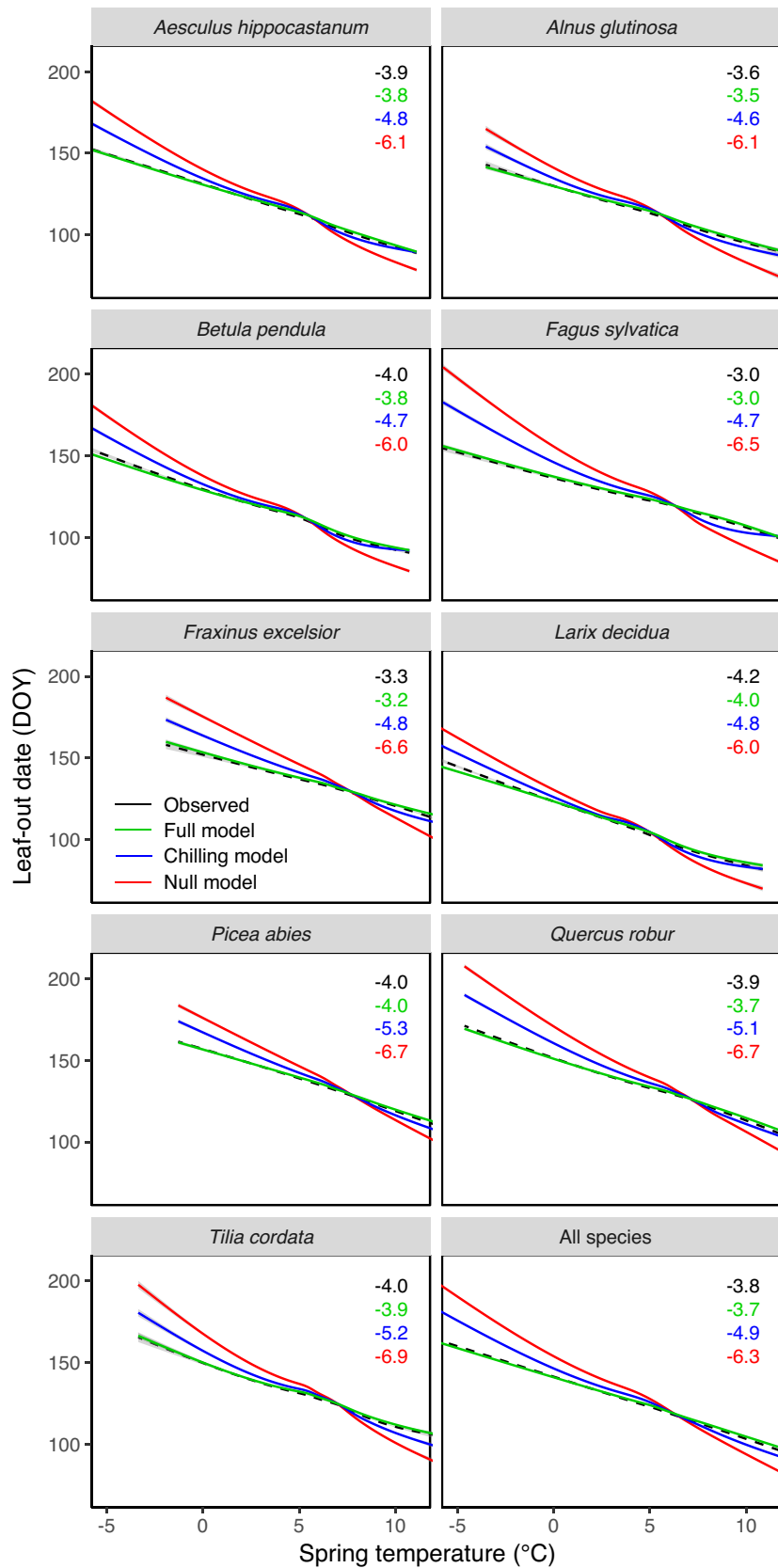
Figure S6 | Spring temperature sensitivities of leaf-out dates. Observed and empirically modelled average leaf-out dates using 10-fold cross-validations in response to spring temperature (observed leaf-out = black lines; *full model* = green lines; *chilling model* = blue lines; *Null model* = red lines). Loess smoothing curves are based on random-effects models to control for differences among sites.
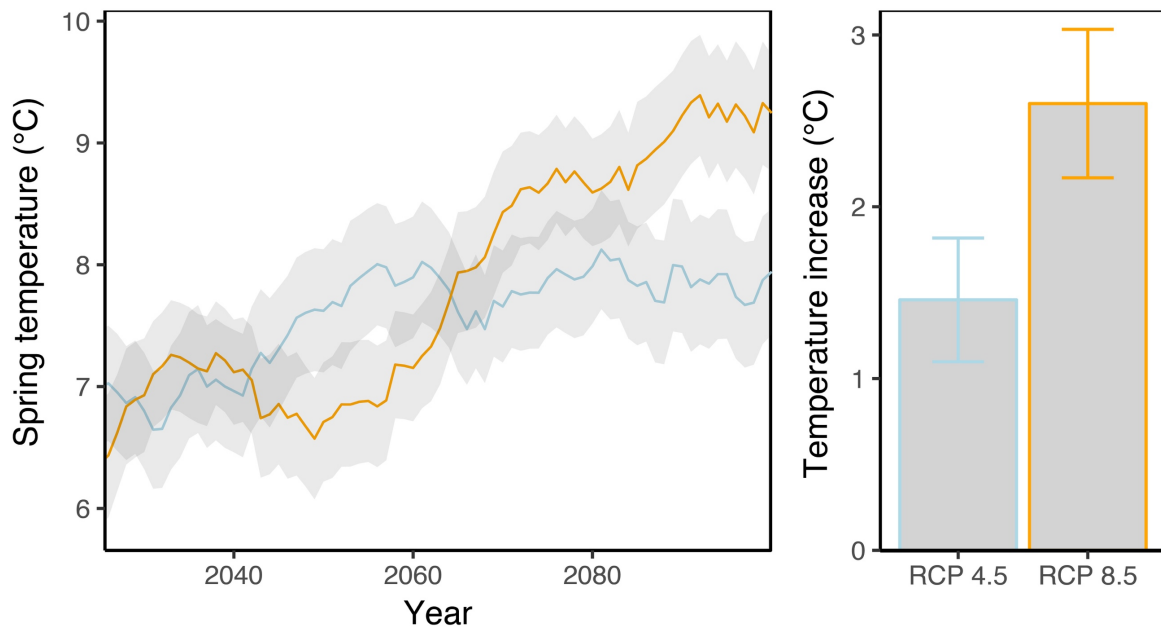
878
879 **Figure S7 | Future projections of Central European spring temperatures. a,** 15-year
880 moving averages for a 'CO$_2$ stabilization' climate scenario (RCP 4.5) (lightblue) or a 'business-
881 as-usual' scenario (RCP 8.5) (orange). The grey area indicates one s.e. either side of the mean.
882 **b,** Estimated increases in spring temperatures by the end of the 21st century compared to 1990–
883 2010. Spring temperatures were calculated as the preseason temperatures 60 days prior to the
884 mean leaf-out date for each individual.
885
886
887
888
889
890
891
892
893
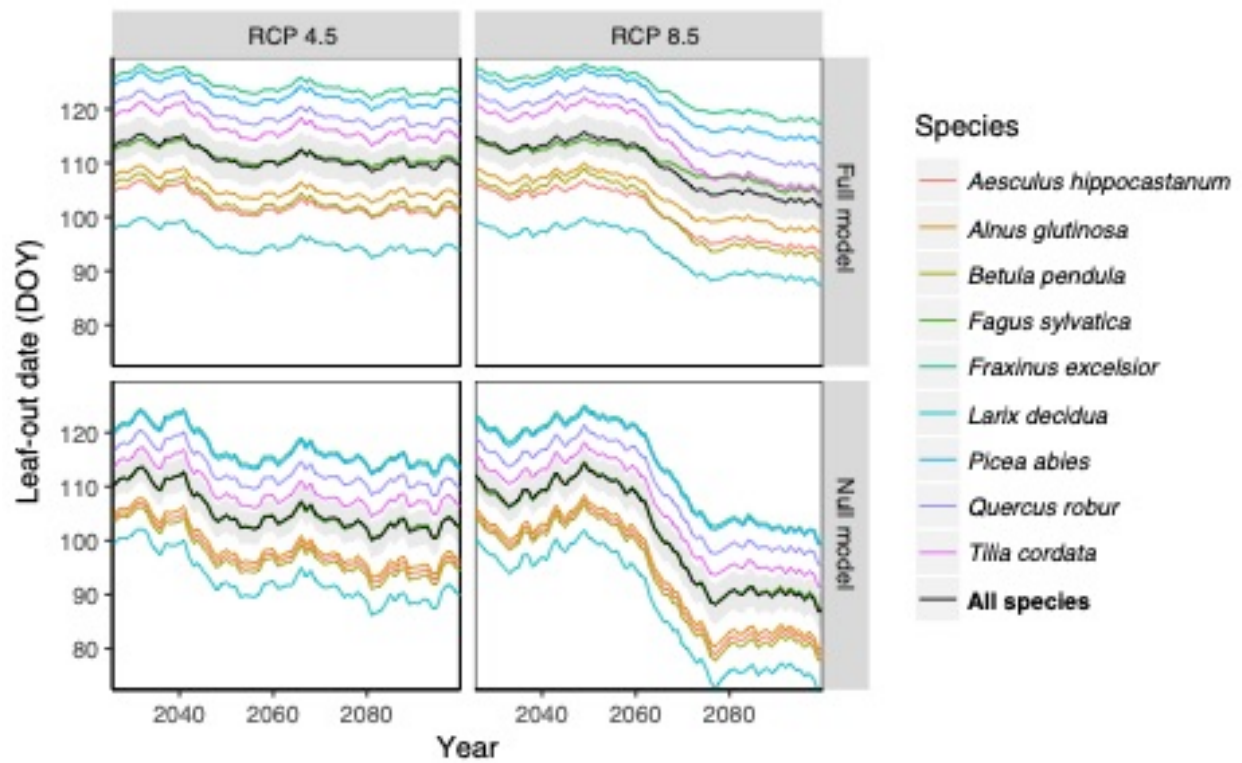
Figure S8 | Future projections of leaf-out dates for the nine study species based on the *full model* (upper panels) or the *Null model* (lower panels) using 15-year moving averages. Left panels: 'CO$_2$ stabilization' climate scenario (RCP 4.5); Right panels: 'business-as-usual' scenario (RCP 8.5). The black line shows the average across all species, the grey area indicates one s.e. either side of the mean.

921
922
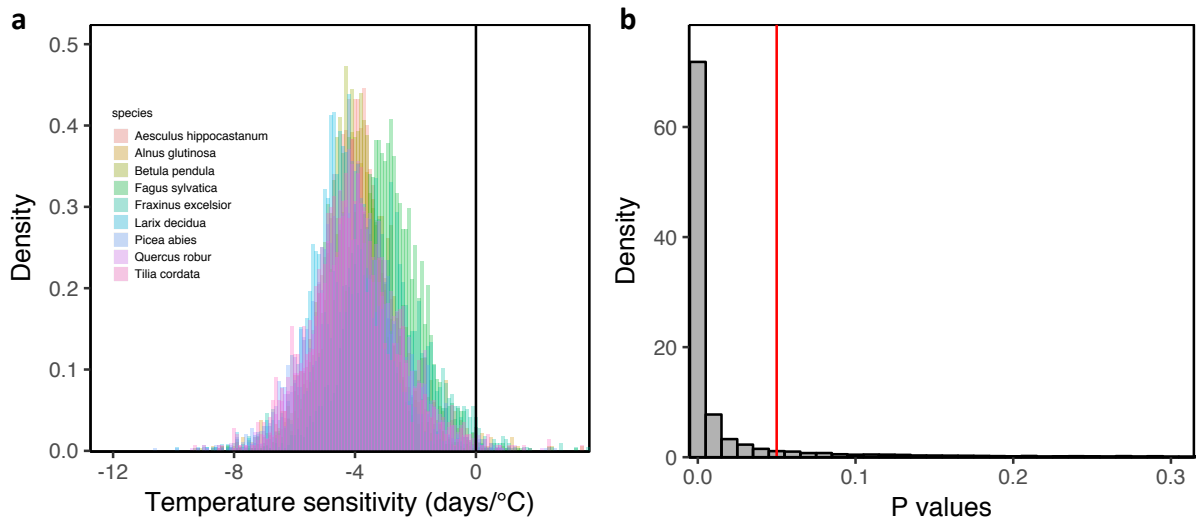
923
924

925 **Figure S9 | Spring temperature sensitivities of the nine study species. a**, Density
926 distributions of spring temperature sensitivities (days advance in leaf unfolding per each °C
927 increase in air temperature) for 24,650 time-series. **b**, Density plot of *P* values for the correlation
928 between spring temperature and leaf-out dates. The red line shows the 5% significance
929 threshold. Number of analysed time-series per species: *Aesculus hippocastanum*, 3703; *Alnus*
930 *glutinosa*, 1841; *Betula pendula*, 3663; *Fagus sylvatica,* 3091; *Fraxinus excelsior*, 2178; *Larix*
931 *decidua*, 2644; *Picea abies*, 2942; *Quercus robur*, 3152; *Tilia cordata*, 1436.

932
933
934
935
936
937
938
939
940
941
942
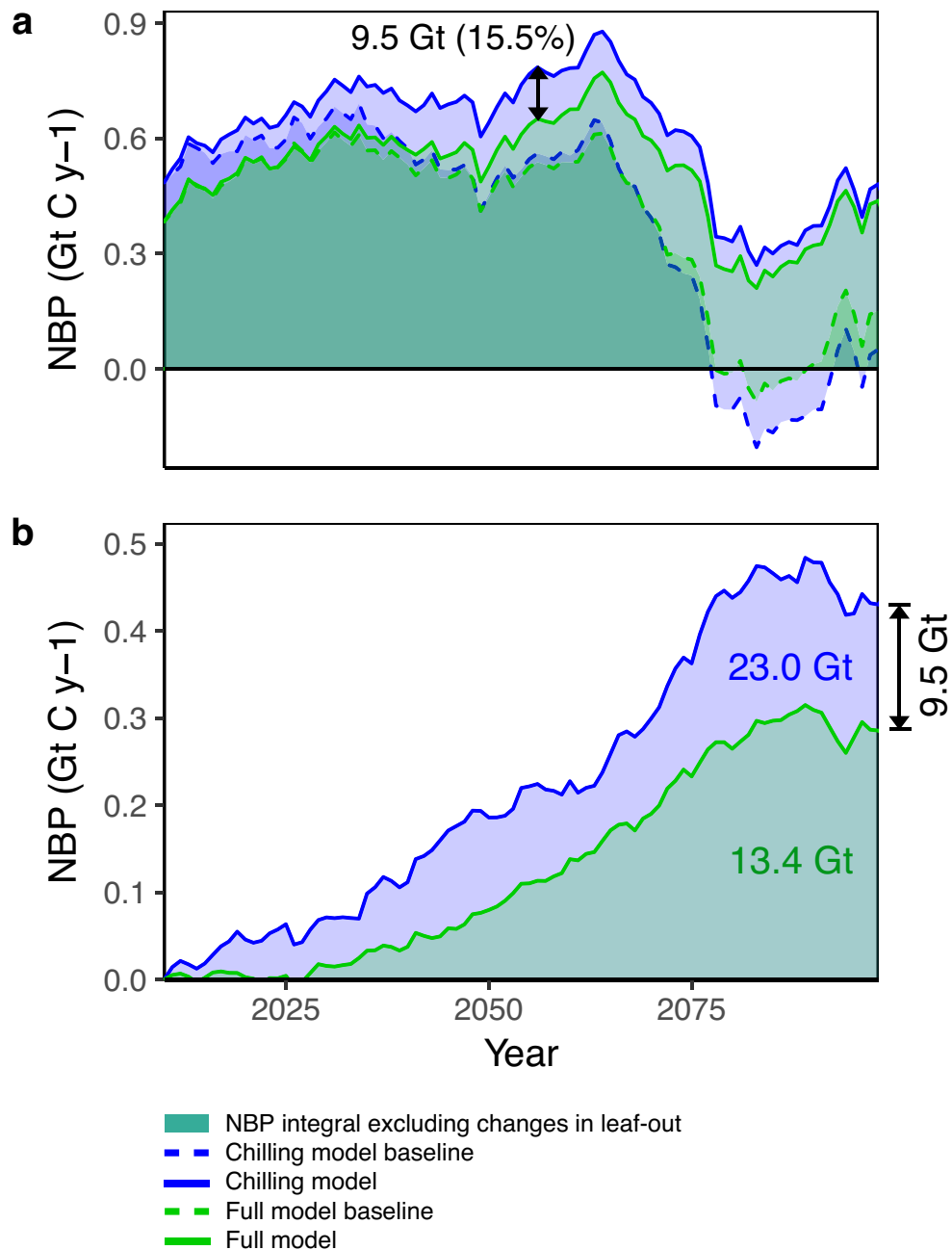
943
944
945 **Figure S10 | Effects of leaf-out changes in Northern Hemisphere temperate forests on net**
946 **biome productivity (NBP). a,** Annual forest NBP (above 23°N latitude) over the 21st century,
947 simulating spring leaf-out times with the *chilling model* (solid blue line) or the *full model* (solid
948 green line). Dashed lines show the baselines assuming no leaf-out changes in the future
949 (phenology fixed at years 2001-2010). **b**, Increases in NBP that are solely caused by leaf-out
950 shifts simulated with the *chilling model* and the *full model*. Arrows show the difference in NBP
951 between the standard LPJ-GUESS model (including chilling-only) and the updated model
952 (including our full phenology model). On average, NBP decreases by 15.5%, which equals a
953 decrease in cumulative NBP over the 21st century of 9.5 Gt.
954
955
956